

# Water-Steam Thermodynamic Equations-of-State from Boyle and Rigidity-Symmetry Lines

Ahmad Eltahlawy<sup>1</sup>, Igor Khmelinskii<sup>1</sup>, Leslie V. Woodcock<sup>2\*</sup>

<sup>1</sup>Department of Chemistry and Pharmacy, University of Algarve, Faro, Portugal

<sup>2</sup>Department of Physics, University of Algarve, Faro, Portugal

Email: \*lvwoodcock@ualg.pt

**How to cite this paper:** Eltahlawy, A., Khmelinskii, I. and Woodcock, L.V. (2025) Water-Steam Thermodynamic Equations-of-State from Boyle and Rigidity-Symmetry Lines. *Journal of Modern Physics*, **16**, 518-535.

<https://doi.org/10.4236/jmp.2025.164027>

**Received:** February 25, 2025

**Accepted:** March 28, 2025

**Published:** March 31, 2025

Copyright © 2025 by author(s) and Scientific Research Publishing Inc. This work is licensed under the Creative Commons Attribution International License (CC BY 4.0).

<http://creativecommons.org/licenses/by/4.0/>



Open Access

## Abstract

We investigate a representation of thermodynamic equations-of-state for water and steam using only physical constants and zero *ad hoc* parameters. Following the reported phase equilibria of a coexisting critical density hiatus and a supercritical mesophase defined by percolation transitions, the state functions density  $\rho(p, T)$ , and Gibbs energy  $G(p, T)$ , of pure fluids are seen to exhibit a symmetry characterised by the rigidity,  $\omega = (dp/d\rho)_T$  along isotherms from the critical point ( $T_c$ ) to Boyle temperature ( $T_b$ ), on either side of the supercritical mesophase for  $T > T_c$ . We report an analysis of H<sub>2</sub>O based upon a knowledge of the lower virial coefficients  $b_2$  and  $b_3$ , that describe the gas region (steam) for all  $T$ . We show that the same coefficients also describe the supercritical liquid-side range “water” in an expansion about a rigidity-symmetry (R-S) line defined by  $\omega(\rho_{RS})_T = RT$  ( $R$  is ideal gas constant). We report further investigation into the Boyle-work line,  $w = p/\rho(\rho_{BW})_T = RT$ . A revised Boyle temperature for H<sub>2</sub>O is reported:  $T_b = 1567 \pm 20$  K. The BW-line is linear in the gas and supercritical liquid regions between  $T_b$  and  $T_c$ . It interpolates to a ground state solid-range constant  $\rho_{BW}(0)$  at an ice density 82.56 mol/l. Cluster expansions in powers of density truncated at  $b_n < b_3$ , equate steam virial coefficients with both BW and RS lines. We find both lines are continuous in all derivatives, and linear within the stable fluid phases. Simple relationships arise from the observation that the higher virial coefficients ( $b_n, n \geq 4$ ) cancel due to cluster equilibria, or are negligible ( $0 < T < T_b$ ) in the steam regions. All thermodynamic state functions  $f(p, T)$  for H<sub>2</sub>O below  $T_b$ , are obtainable from the critical ratio of virial coefficients  $-(b_2/b_3)_{T_c}$  determined from the linear Boyle line given only one H<sub>2</sub>O  $\rho_{BW}(0)$  ground-state density physical constant.

## Keywords

Liquid-State Theory, Cluster Physics, Fluid Thermodynamics, Boyle Line,

## 1. Introduction

### 1.1. Continuity Hypothesis

It is over 150 years since the birth of classical thermodynamics, whence J. W. Gibbs published his description of thermodynamic properties, and transitions between different phases, as state functions on 2-dimensional, e.g. temperature ( $T$ ) and pressure ( $p$ ), surfaces [1]. In that same year, van der Waals PhD thesis [2] introduced the concepts of a theoretical equation-of-state  $p(V, T)$  for pressures of a gas at fixed  $V$  (volume) and  $T$ , based upon his hypothesis that there exists a singularity described by the node of a cubic equation. Van der Waals' equation-of-state defines a hypothetical critical temperature  $T_c$ , pressure  $p_c$ , and singular volume  $V_c$  at the "critical point". For all  $T > T_c$  and all  $p > p_c$ , there is no supercritical delineation between gas and liquid states in van der Waals in gas-liquid "continuity" theory. All points on a Gibbs  $V(p, T)$  surface are defined by state functions of  $p$  and/or  $T$ . If the hypothetical critical point defined by van der Waals equation existed, it would be an exception to the phase rule of Gibbs.

Given the equilibrium-state heat capacity at constant pressure ( $C_p$ ) Gibbs defined both enthalpy ( $dU + pdV = C_p dT$ ) and entropy ( $dS = C_p d \log_e T$ ). Then, "enthalpy is a state function", and "entropy is a state function", are concise statements of the 1<sup>st</sup>- and 2<sup>nd</sup>-laws of classical (reversible) thermodynamics, respectively [3].

Every thermodynamic state ( $p$ - $T$ ) point on a Gibbs surface is defined where two lines cross and characterised by the number of degrees of freedom ( $F$ ) in its specification by Gibbs phase rule. For a one-component system ( $C = 1$ ) then, for  $P$  phases in coexistence,  $F = C - P + 2$ . All single-phase state points when ( $F = 2$ ) are defined when an isotherm crosses an isobar, *i.e.*, by  $T, p$ . A state point in a two-phase region ( $F = 1$ ) is defined when either an isotherm or an isobar crosses a coexistence line. The coexistence lines are defined by the intersection of lines of chemical potential ( $\mu$ ), on the  $\mu(p, T)$  surface. The triple-point densities are defined by the intersection of two coexistence lines. There is no thermodynamic definition of a hypothetical critical density singularity [4].

### 1.2. Universality Hypothesis: Water-Steam

Another hypothesis that has been fashionable amongst theoretical physicists for about 50 years is the concept of universality [5]. From Ising models, ferro-magnetic systems, spin glasses, to liquid-gas criticality. According to this doctrine, all critical phenomena obey the same universal scaling description, in the vicinity of a hypothetical "critical point", which is explained using group renormalization theory. The originator of this theory, K. Wilson, summarized the phenomenology of liquid-gas criticality by reference to water and steam in an introductory paragraph as follows [6]:

“A critical point is a special example of a phase transition. Consider, e.g. the water-steam transition. Suppose that water and steam are placed under pressure always at the boiling temperature. At the critical point, the distinction between water and steam disappears, and the whole boiling phenomena vanishes. The principal distinction between water and steam is that they have different densities. As the pressure and temperature approach their critical values the difference in density between water and steam goes to zero.”

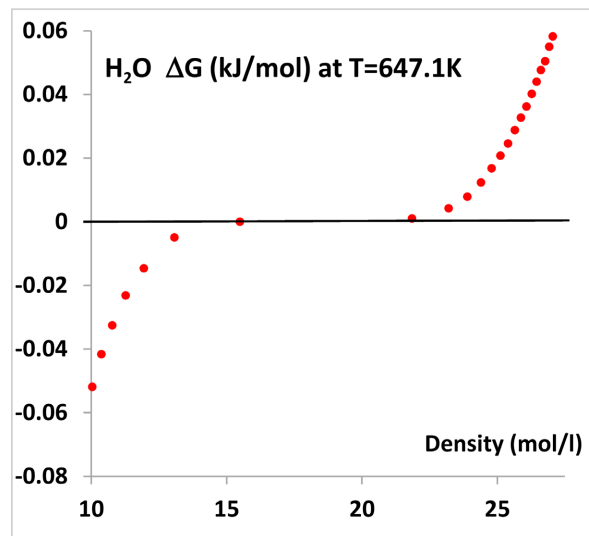


**Figure 1.** Gibbs energy of water along the critical isotherm relative to critical pressure ( $T_c, p_c$ ) state point (NIST 2025 [7]) showing the critical density hiatus whence  $\rho dG(T) = dp = 0$ , to within an experimental uncertainty; estimated maximum coexisting gas density is 15.50 mol/l and minimum coexisting liquid density 21.85 mol/l: the plot is indicative of the symmetry of thermodynamic state functions between gas and liquid on either side of the critical divide.

It is evident from modern 5-figure precision Gibbs energy data shown in **Figure 1** [7] [8], that Wilson’s Nobel address opening statement about water does not accord with the latest water-steam thermodynamic data compilations [9]. Investigations of percolation transitions in model square-well fluids [10], and many model and real fluids since Wilson [5] [11], have also discredited this hypothesis. At the critical temperature  $T_c$  the density difference does not go to zero. A liquid-gas critical “point”, as hypothesised by van der Waals and accepted by the physics community for 150 years, does not exist as such. Moreover, there is no universality of critical phenomena that spans the diversity of 2- and 3-dimensional critical phenomena systems as hypothesized [6]. The statistical thermodynamic description of percolation transitions is fundamentally different in 2D compared to 3D [5].

### 1.3. Percolation Lines PB and PA

In the  $\rho(T, p)$  surface there is a dividing line of uniform chemical potential connecting maximum and minimum coexisting gas and liquid densities, respectively (**Figure 2**). Above this critical divide at  $T_c$ , there exists a supercritical mesophase

bounded by weak higher-order percolation transitions below which there is the familiar liquid-vapour coexistence region.

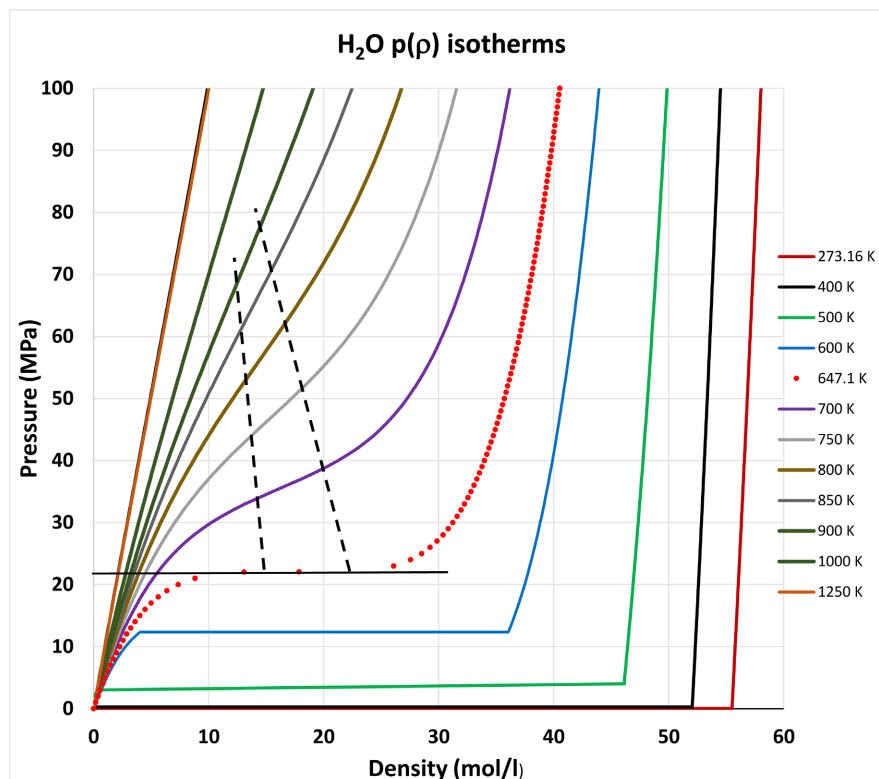


**Figure 2.** Experimental data points for the  $p(\rho)_T$  isotherms of supercritical water from NIST [7] [8] <https://webbook.nist.gov/chemistry/fluid/>; the horizontal black line is a critical pressure 22.06 MPa; the dashed lines are percolation lines at  $T_c$  show the maximum steam (PB) and minimum water (PA) coexisting densities, respectively.

**Figure 2** shows that water and steam exhibit essentially the same phenomenology as fluid phases of argon [10] [11]. The isotherms show there is a gas region with the percolation of bonded clusters (PB) and liquid like delineated by percolation of gas voids (PA) as shown. At supercritical temperatures, one Gibbs phase of water or steam states exist with distinct liquid and gas properties and are separated by a supercritical mesophase. The near critical mesophase can be characterized as being macroscopically homogeneous, but microscopically heterogeneous colloidal-like mixture of gas-like monomer molecules and molecular clusters, and liquid-like macroscopic clusters, all species with the same Gibbs chemical potential. These phase boundaries appear as weak higher-order thermodynamic phase transitions within a single phase ( $F = 1$ ) on the Gibbs  $p$ - $T$  surfaces. They were unforeseen by Gibbs but recently have been shown to play a role in determining a phase diagram in accord with Gibbs phase rule [4] [5].

#### 1.4. Water Equations-of-State

In order to reproduce the experimental measurement precision, modern equa-

tions-of-state, require more than 100 adjustable parameters. In the case of water and steam it is 148 [9]. In **Figure 3** we show a schematic plot of sub-phase regions from reference 7 that divides up the Gibbs fluid phase for the water equations-of-state into areas that are amenable to different functional representation. The 5 regions shown correspond to region 1 - 34 parameters (steam), region 2 - 52 parameters “water” both sub and supercritical, with no delineation, 3 - 40 parameters supercritical mesophase, 4 - 10 parameters subcritical gas-liquid coexistence, and region 5 - 12 parameters an arbitrary high temperature (low density) region 1073 - 2023 K to 50 MPa: total number of parameters is 148. The authors report an empirical equation-of-state for each region together with several *ad hoc* adjustable fitted parameters. The regions can be understood with reference to the phase diagram of water and steam, however, given present knowledge of supercritical mesophase and its delineation by the supercritical fluid states percolation lines PB and PA [5] [10] [11].

Our objective is to obtain an equation-of-state of water and steam with only scientific physical constants and zero adjustable parameters. This should be achievable over the whole  $p$ - $T$  range of existence of experimental  $p$ - $\rho$ - $T$  data up to the Boyle line, shown in **Figure 2**, to maximum pressure of 250 MPa, and perhaps even beyond. The NIST data bank [9] accurate experimental  $\rho(p, T)$  data for steam regions up to 1000 MPa.

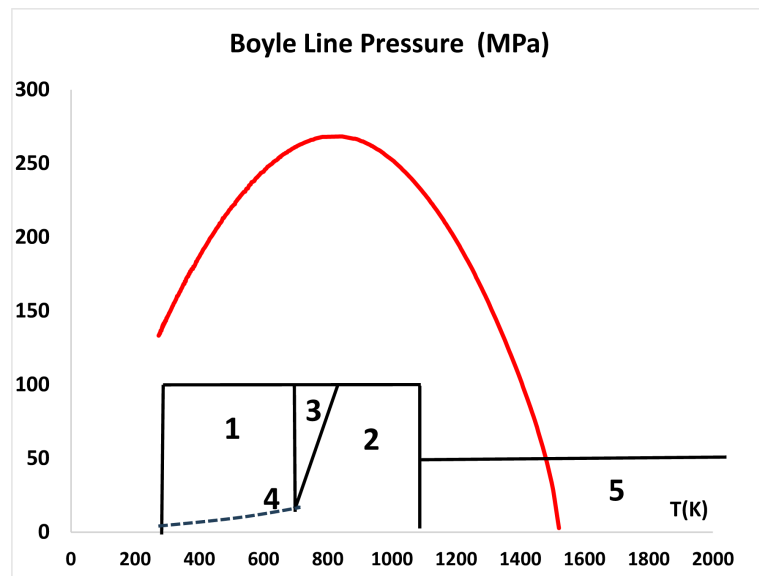


**Figure 3.** Pressure of steam along the Boyle line (red), for which  $p/\rho = RT$ , obtained from the NIST data values [7] [8] between  $T_i$  (273 K) and the Boyle temperature ( $T_B$ ); the black lines of the  $p$ - $T$  plot for  $H_2O$  delineate the regions and range of the numerical equations-of-state of Kretzshmar and Wagner [9] (Fig. 22 on page 11) for the assignment of basic equations to the 5 regions of IAPWS-IF97.

The NIST-data Boyle line for the pressure is seen to be a quadratic, terminating around 1550 K, *i.e.* at  $T_B$  and peaking at  $T_B/2$  and interpolating to 0 at 0 K. This Boyle-line behavior was first investigated and analyzed by Powles for several pure

fluids [12]. Since the pressure line  $p(T)$ , for the condition  $p/\rho = RT$ , is quadratic, substituting  $p = \rho_{\text{BW}}RT$  for the Boyle-work density line, we obtain  $\rho_{\text{BW}}(T)$  for water to a temperature slightly below  $T_c$ , is linear (Figure 4). This “obscure” result was reported as such, by Powles, but the linearity has hitherto remained inexplicable. It is not found to be linear when the Boyle line (sometimes referred to as the zero line) is obtained for equilibrium crystal regions, for example [13].

## 2. Boyle Work (BW) and Rigidity Symmetry (RS) Lines

### 2.1. Boyle Work Line

First, we report a revised determination of the Boyle temperature ( $T_B$ ), and Boyle-work (BW) line ( $p/\rho_{\text{BW}} = RT$ ) with high precision. It is seen to be a perfectly linear function of density and subject only to variations in the inaccuracy of the experimental data points. This linearity for  $p/\rho = RT$  on the  $T(\rho)$  plot (Figure 4) for  $\text{H}_2\text{O}$  from NIST [9] accords with the perfect quadratic parabola for the pressure of the Boyle line for  $T > T_c$  shown above in Figure 3.

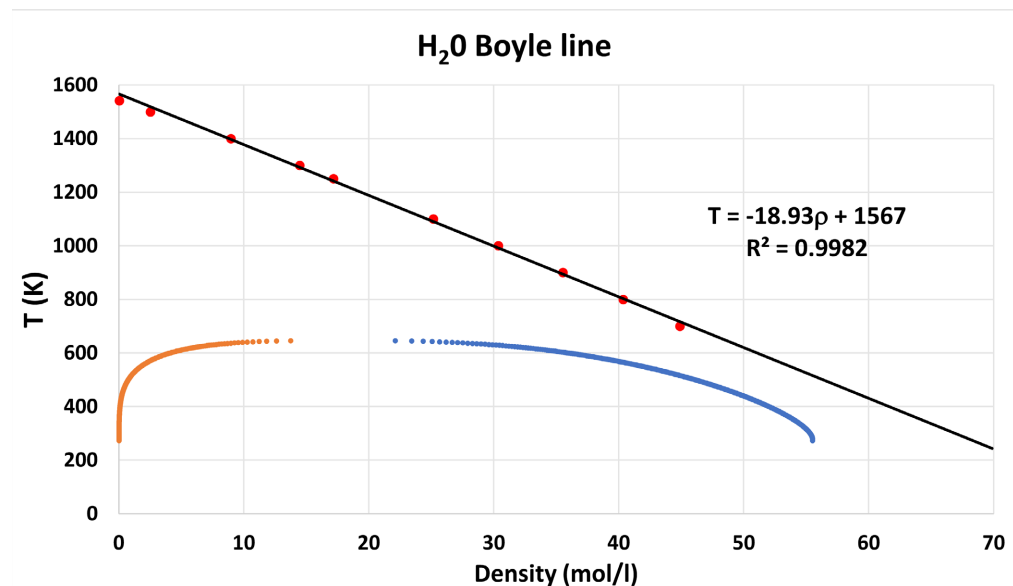


**Figure 4.** Boyle-work (BW) line for water (black) obtained from 10 fluid state data points taken from the NIST Thermophysical Properties (water) [9], shown in comparison to the 2-phase steam-vapor (red) water (blue) coexistence envelopes also from NIST data [9]: the Boyle line is taken to be the same as EXCEL trendline with the constants and regression shown.

Both steam Boyle temperature and a ground-state “solid” constant of the water Boyle-work line can be obtained from the EXCEL trendline equation in Figure 4. We obtain  $T_B = 1567$  K and  $\rho_{\text{BW}}(0) = 82.8$  mol/l from the EXCEL trendline.

If the BW line were to be perfectly linear, an alternative determination requires only one high resolution state point  $\rho_{\text{BW}}(T)$  along any isotherm. We obtain  $\rho_{\text{BW}}(0)$  values of 80.32 and 83.90 mol/l for  $T = T_c$  and 1000 K isotherms respectively. Figure 5 shows a plot of the Boyle-work lines for the two isotherms 647.1 K ( $T_c$ ) and 1000 K reduced by  $RT$ . The most striking aspect of these plots is the symmetry

between steam and water states on either side of the mesophase when a trendline quadratic is fitted. If this symmetry were to be perfect, it explains the linear dependence of  $\rho_{BW}(T)$  at  $w/(RT) = 1$ .

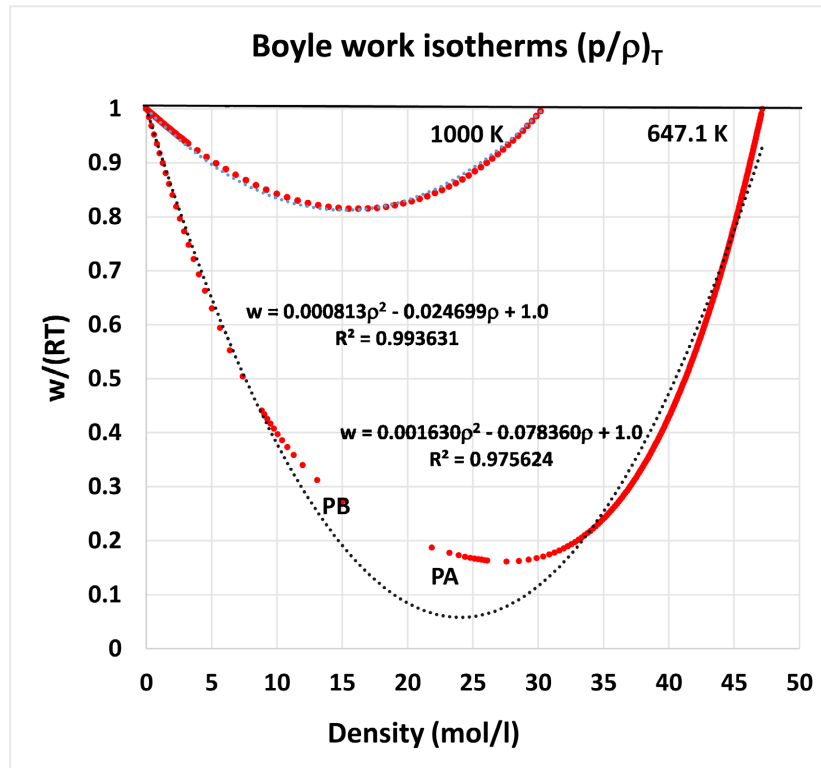


**Figure 5.** Reduced experimental work ( $w$ ) ratio ( $p/\rho RT$ ) along the critical isotherms 647.1 K ( $= T_c$ ) and 1000 K (NIST data from reference [7]): the percolation line PB (gas clusters) and PA (liquid voids) correspond to the maximum coexisting gas density  $(\rho_{PB})_{T_c}$  and minimum coexisting liquid density  $(\rho_{PA})_{T_c}$  along the critical isotherm: the dashed lines are EXCEL quadratic trendlines showing symmetry of isotherms centered on PA but deviating from NIST data in vicinity of critical coexistence.

The conclusion to be drawn from **Figure 5** is that the excellent quadratic fit for both the gas side and the liquid side of the  $p/\rho$  isotherms,  $w(\rho)$ , for all  $T$  from  $T_c$  to  $T_b$  is that  $w/(RT)$  is symmetric and a quadratic function of density, and that only two coefficients are required to determine the equation-of-state  $p(\rho)_T$  plus the BW line density  $\rho_{BW}(T_b)$  at  $w/(RT) = 1$ . If we define a density difference  $\Delta\rho = (\rho_{BW} - \rho)_{T_b}$  then we can see that the linearity of  $r_{BW}$  in the limit  $T \rightarrow T_b$  extends to  $T_c$  given (i) the quadratic relationship between gas side and supercritical-liquid side of  $w/(RT)$  in **Figure 5**, and (ii) knowing that the linearity of  $\rho_{BW}(T)$  has also been found to be accurate over the range  $T_b > T > T_c$  for argon [12].

### 2.2. Rigidity-Symmetry Line

Rigidity  $(\omega)_{p,T}$  is a defining state function that describes the distinction between gas states below the Boyle temperature and liquid or solid states [14] [15]. It is a reciprocal compressibility that also relates to Gibbs energy, and hence also to den-

sity fluctuations, by the following equalities of classical thermodynamics and Boltzmann statistics in the theory of simple liquids [16]

$$\omega = \left( \frac{dp}{d\rho} \right)_T = -\frac{V}{K_T} = V \left( \frac{dp}{d \ln V} \right)_T = \rho \left( \frac{dG}{dp} \right)_T = \left( \frac{d\mu}{d \ln N} \right)_{V,T} = RT / \left( \langle \Delta N^2 \rangle \right)_{V,T} \quad (1)$$

where  $K_T$  is the isothermal compressibility,  $G$  is Gibbs energy,  $\mu$  is Gibbs chemical potential and  $(N/V)$  is a number density. It decreases with density for a gas and increases with density for a liquid or solid. The last equality reveals the statistical origin is density fluctuations that are determined by fluctuations of liquid-like clusters of molecules in gas, that are mirrored by fluctuations of gas like voids or monomers in corresponding liquid states, of same rigidity.

It is the symmetry of the rigidity, that reveals the connection to percolation transitions that can define the distinction between gaseous states, and liquid or solid states below the Boyle temperature. Accurate rigidity data have been used, *inter alia*, to invalidate hypotheses that assume all real gas-liquid critical points exist as a singularity with universal scaling laws [5].

A similar line to  $\rho_{BW}(T)$  can be defined as the rigidity symmetry (RS) line:  $\rho_{RS}(T)$  connects all  $\omega = RT$  state density points on the liquid side of supercritical isotherms at a somewhat lower density than  $\rho_{BW}(T)$ , *i.e.* when the  $\omega(\rho, T)$  state point has the same rigidity as the ideal gas *i.e.*  $\omega = RT$ . In the following sections we will relate the RS line to the BW line and to the two percolation lines for water or steam as found previously for argon [15]. It is this symmetry between the steam densities below  $\rho_{PB}(T)$ , and water-like densities between  $\rho_{PA}(T)$ , and the rigidity symmetry (RS) line  $\rho_{RS}(T)$ , that can explain the linearity of both  $\rho_{BW}(T)$  and  $\rho_{RS}(T)$ .

For pure fluids, rigidity,  $\omega(T)$ , can be obtained from the heat capacity data in NIST thermophysical webbook [7], given the speed of sound ( $c$ ) values and the heat capacity ratio, then  $\omega = c^2 C_p / C_v$ . The rigidities of isotherms below  $T_B$  to  $T_c$  are shown in **Figure 6**.

As with the Boyle line for various fluids [12], the water rigidity line (black) shown is linear, the same as fluid argon [12] [15]. An inspection of the  $\omega(T)$  isotherms in **Figure 6** shows a symmetry that is consistent with the existence of a supercritical mesophase within which it remains constant along any isotherm and decreases from  $RT_B$  at the Boyle temperature: defined as in **Figure 4**, as the isotherm above which there is no negative minimum in  $p/(\rho RT) - 1$ . The rigidity ( $\omega$ ) is everywhere positive for equilibrium fluid states and decreases to zero within the critical divide at  $T_c$  (**Figure 6**).

Notwithstanding the known complexities of the steam-water molecule, and the quantum effects of the H-bonds in cluster and solid structures, the thermodynamic equations-of-state for water reveals a near perfect steam-water rigidity symmetry, and hence also a linear  $\rho_{RS}(T)$  line as previously reported. The data, illustrated in **Figure 5** and **Figure 6**, can be obtained from NIST tabulations [7] which has been calculated from the Wagner-Pruss (W-P) equation-of-state [8] to represent the experimental thermophysical fluid data to within an accuracy that it has been reportedly measured. We only need an accurate description of the

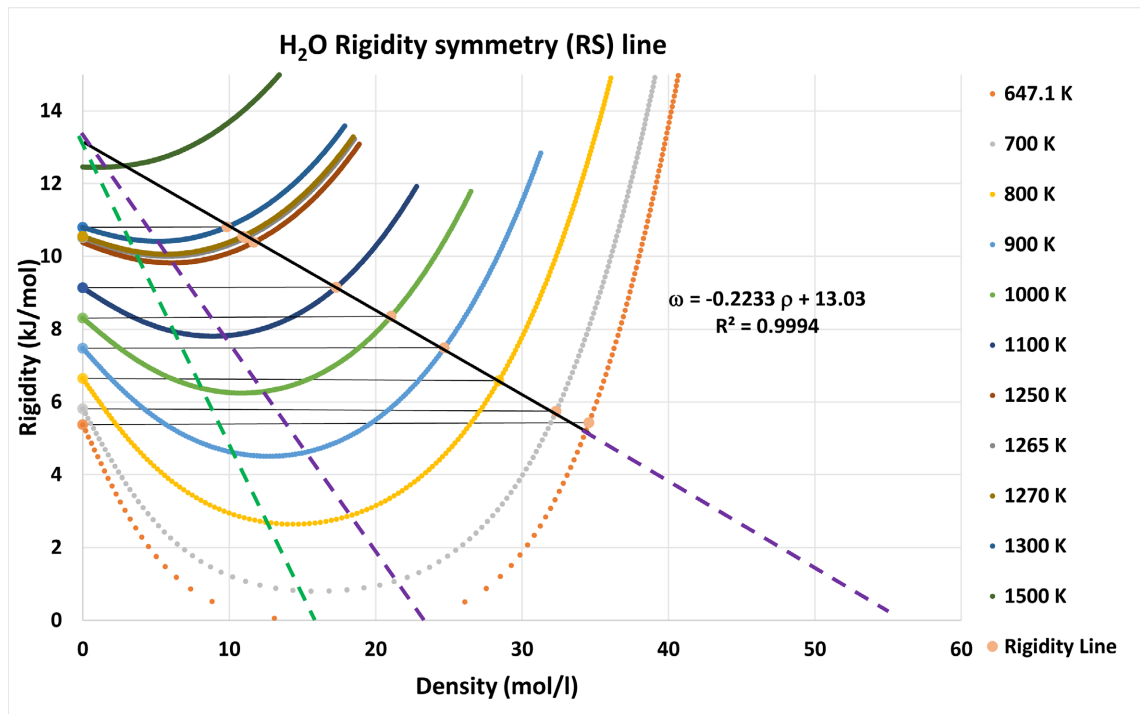


**Figure 6.** Plots of  $(dp/d\rho)_T$  (rigidity) for lower supercritical isotherms obtained from the NIST Thermophysical Properties of Fluids: water [7] showing the symmetry between steam in the ideal gas low-density limit for steam, and supercritical “water”: corresponding states are connected by the horizontal thin black lines.

equilibrium low-density steam phase to also describe the high-density water phase with the same precision. In this region, a two-term virial equation with only  $b_2(T)$  and  $b_3(T)$  terms suffices.

### 2.3. Virial Equations for Steam and Water

Given the scientific description of the phase transitions, the percolation lines PB and PA, and the BW and RS lines, this number of adjustable parameters can be reduced to zero, without loss of precision, using just the necessary physical constants. This requires the virial coefficients along any isotherm. From **Figure 6** we infer that  $p(\rho, T)$ , of steam below  $T_B$ , for all densities below the percolation transition density  $\rho_{PB}(T)$ , will be continuous in all derivatives, and represented by the Mayer virial expansion for the pressure in powers of density along an isotherm [16]

$$p = \rho RT \left( 1 + b_2 \rho + b_3 \rho^2 + \dots + b_n \rho^n + \dots \right) \quad (2)$$

The experimental pressure is evidently continuous in all its derivatives up to the first discontinuity, *i.e.* percolation line PB, whereupon the functional form changes as  $\omega(T) = (dp/d\rho)_T$  remains constant for the narrow density range within the mesophase from PB to PA.

Given the rigidity symmetry seen in **Figure 6**,  $p(\rho, T)$  for water state points for densities exceeding PA can be obtained from the same virial expansion coefficients used to describe steam isotherms at the higher densities above  $\rho_{PA}(T)$  and

for densities below the RS line on any isotherm in an expansion in powers of the density difference  $\Delta\rho_{RS} = (\rho - \rho_{RS})_T$ . The functions  $p(\rho)_T$  and  $p(\Delta\rho_{RS})_T$  are empirically quadratic for all  $T < T_B$ . The same virial coefficients that describe the gas phase for densities below the PB line can be used to represent the  $p(\rho, T)$  data for the supercritical liquid region between  $T_c$  and  $T_B$  for densities between the PA and RS lines at, and above the PA line, *i.e.*  $\rho_{PA}(T)$ . All known experimental supercritical isotherms extend to higher temperatures, up to  $T_B$  (=1567 K) for steam, and pressures to 1000 MPa [7].

The liquid region between  $T_c$  and  $T_t$  is amenable to expansion around the BW line  $\rho_{BW}(T)$  along any isotherm. The high-density liquid-side pressure equation-of-state  $p(\rho, T)$  can be obtained from the rigidity isotherms, via the equalities in Equation (1) for all  $T < T_B$ . Other thermodynamic state functions, *e.g.* Gibbs energies that determine phase coexistence boundaries can subsequently be prescribed in terms of the various physical constants for water at temperatures up to  $T_B$  (1567 K) and 1000 MPa [15]. Real gases are composed of clusters of atoms or molecules, even at very low finite densities, to some extent, for all temperatures below  $T_B$ .

In the following section we show how the equilibrium constants between molecular clusters and monomer molecules relate to the virial coefficients that determine the  $p(\rho)_T$  that enable the equations-of-state to be prescribed without any adjustable parameters other than physical constants determined from the available experimental  $p(\rho, T)$  data, and the second virial coefficient from the triple point ( $T_t = 273.16$  K) to  $T_B$  (1567 K) for  $H_2O$ .

### 3. Cluster Equilibria

#### 3.1. Equilibrium Constants

Steam in any equilibrium thermodynamic state below  $T_B$  is a multicomponent mixture of monomers, dimers, trimers etc. This general revision of cluster physics of all real gases was first suggested by Sedunov [17]. Each species obeys the ideal gas law of partial pressures in the low-density limit. The equilibrium constants  $k_n$  for multiple association can be expressed as sequence of gas phase chemical reactions according to the equilibria:  $n(H_2O) \rightleftharpoons (H_2O)_n$ . The total pressure can be expanded as a series when  $(H_2O)_1$  is the monomer mole fraction and  $(H_2O)_n$  fraction of cluster size  $n$ . Defining the equilibrium constants,

$$k_n = (H_2O)_n / (H_2O)_1^n \quad (3)$$

Using the square brackets for densities, the Dalton-law partial pressures can be summed as a series for the cluster particle density species  $n(\rho_p)$  at total pressure ( $p$ ),

$$p = \rho_p RT = 1 + k_2 [(H_2O)_1]^2 + \dots + k_n [(H_2O)_1]^n + \dots \quad (4)$$

$$\text{and } \rho = [(H_2O)_1] + 2k_2 [(H_2O)_1]^2 + \dots + nk_n [(H_2O)_1]^n + \dots \quad (5)$$

From Equations (4) and (5) the equilibrium constant between monomers and

dimers relate to the Mayer virial coefficients:  $k_2 = -b_2$  and for trimers  $k_3 = (2k_2)^2 - b_3$  are obtained. These simple relations between  $b_n$  and  $k_n$  [5] [17] show there is a significant cancellation, to some unknown extent, of the higher virial terms in the Mayer cluster expansion Equation (2). All higher virial coefficients contain a dependence upon  $k_2$  and  $k_3(T)$ . We find that for all steam equilibrium state points for  $T < T_B$ , only  $b_2(T)$  and  $b_3(T)$  are required for accurate pressures in the range from  $T_B > T > T_c$  at densities below the percolation line  $\rho_{PB}(T)$ , and for all isotherms below  $T_c$ , and for all equilibrium gas states at densities below both the gas-liquid and gas-solid coexistence line. This delineated (by PB) definition, and empirically accurate simplification of the gaseous state below  $T_B$ , requiring only  $b_2(T)$  and  $b_3(T)$ , has also been found to apply to gaseous argon [15].

### 3.2. Virial Coefficients of Steam

There is an extensive literature on the second- and third-virial coefficients of steam although there is a dearth of original data for  $b_3(T)$ , notwithstanding many computer-model pairwise Hamiltonian predictions. The most comprehensive data for  $b_2(T)$  from experimental data is by Harvey and Lemon [18]. The experimental correlation they report up to  $T = 1273$  is parameterised in an equation that extrapolates to  $b_2 = 0$  at the Boyle temperature, using a guidance from model pair potential computer calculations. They obtain a value of  $T_B = 1538$  K, that compares favourably with our result from the 2024 NIST Boyle-line interpolation in **Figure 4** ( $T_B = 1567$  K). A combined uncertainty of less than  $\pm 2\%$  could accommodate both results. We have recalculated the values of  $b_2(T)$ , and from the NIST isotherms using a parameterisation of  $p(\rho)_T$  in the range from  $T_i$  to  $T_B$  the results are plotted in **Figure 7**.

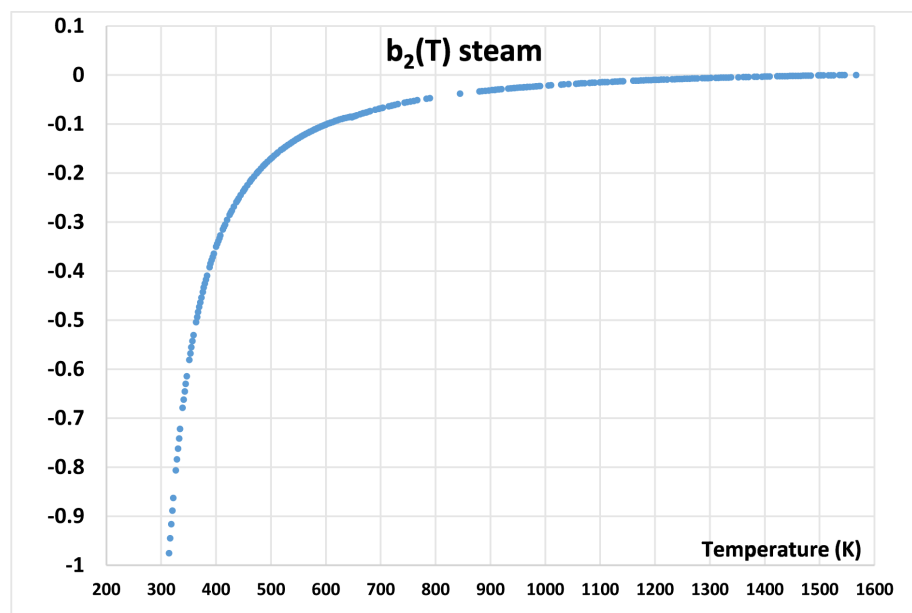


**Figure 7.** Steam second virial coefficient  $b_2(T)$  in units of  $10^{-3}$  (l/mol) obtained from NIST  $p(\rho, T)$  data [9] for  $\sim 250$  isotherms from  $T = 300$  K to  $T_B(1567)$ .

The Mayer virial series Equation (2), is a Taylor expansion for pressure derivatives in powers about zero density, whence “bond” lengths within clusters that determine  $k_n$  become negligible compared to divergent correlation lengths between clusters that determine  $p(\rho)_T$  in the virial expansion Equation (2). The rigidity symmetry along an isotherm means that the liquid-side supercritical properties can be determined from the corresponding-state gas phase given only these lower virial coefficients. We can now proceed to specify the thermodynamic state functions. notably, the Boyle and critical and triple point temperatures, BW and/or RS lines, and the coexisting PB and PA densities at  $T_c$  by physical constants required to specify the delineation lines between equations for  $p(\rho)_T$  from  $T_t$  to  $T_B$ .

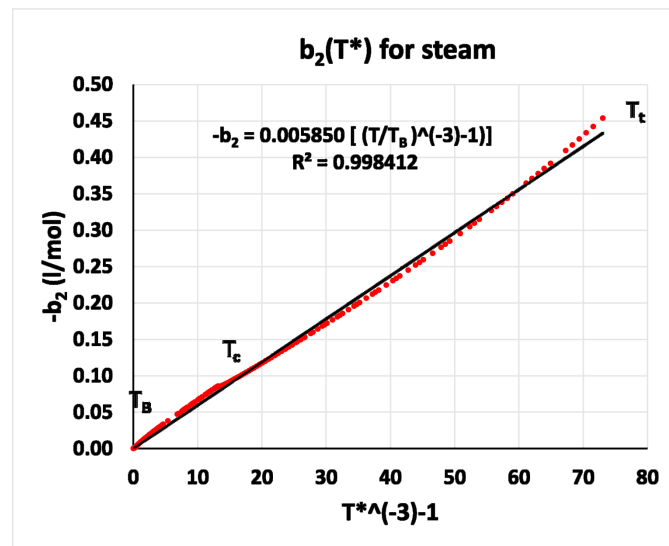


**Figure 8.** Dependence second virial coefficient,  $b_2(T)$ , on reduced temperature  $(T^*)^{-3}$ ; reduced temperature  $T^*$  is defined as  $T/T_B$ .

The best available data, including our own data for  $b_2(T)$  is shown in a reduced form in **Figure 8** and is amenable to a linear parametrisation with a single parameter over the entire range from Boyle  $T_B$  to triple-point  $T_t$ . Preliminary results for  $b_3(T)$  [19], show that for steam-water above  $T_c$ , as with argon [15], shows a maximum  $b_2(T)$  and  $b_3(T)$  confirm a linear relationship to the BW line for  $T > T_c$  by  $-b_2 = b_3 \rho_{BW}(T)$  exactly in the limit  $T \rightarrow T_B$  as noted by Powles 40 years ago [12].  $b_3$  and also  $b_4$ , that goes to zero at  $T_c$ , appear to contain information on  $T_c$ .  $b_3(T)$  shows a maximum at  $T_c$ , whereas  $b_4$  goes to zero for all  $T > T_c$ . The higher virial coefficients  $n > 4$  must either cancel, similarly, or will become negligible at the low densities below the  $\rho_{PB}(T)$  line. Hence, we can proceed to specify the requisite physical constants for thermodynamic equations-of-state from only the lower virial coefficients  $b_2(T)$  and  $b_3(T)$  for all gaseous states below  $T_B$ .

### 3.3. Relation of $b_2/b_3$ to PB, PA Lines

The percolation pressures, of bound clusters in the gas, and of gaseous voids in the liquid, with decreasing  $T$ , intersect to trigger a critical point coexistence line

at  $T_c$  and a supercritical mesophase with linear hybrid properties in the mesophase. The percolation transitions are higher-order phase transitions that delineate the gas phase below the Boyle temperature when the clusters of “liquid-in-gas” diverge to percolate the phase volume. There are no phase transitions for all gas densities below the PB-line density  $\rho_{PB}(T)$ . The gas phase equation-of-state is given by the Mayer virial expansion, for given  $T$ . For all  $\rho < \rho_{PB}(T)$ , we have the following, formally exact virial series, up to the first thermodynamic discontinuity, virial expansions to describe the BL and RS lines and  $(d\omega/d\rho)_T$  “solidity” line [5] [15]).

$$\text{work} \quad w = \left( \frac{p}{\rho} \right)_T = RT \left( 1 + b_2 \rho + b_3 \rho^2 + \dots + b_n \rho^{n-1} \right) \quad (6)$$

$$\text{rigidity} \quad \omega = \left( \frac{dp}{d\rho} \right)_T = RT \left( 1 + 2b_2 \rho + 3b_3 \rho^2 + \dots + nb_n \rho^{n-1} \right) \quad (7)$$

$$\text{solidity} \quad \sigma = \left( \frac{d^2 p}{d\rho^2} \right)_T = RT \left( 2b_2 + 6b_3 \rho + \dots + n(n-1)b_n \rho^{n-2} \right) \quad (8)$$

The Boyle work ratio for both the critical isotherm (647.1 K) and  $T = 1000$  K, of  $H_2O$  in **Figure 5** show that both work ( $w$ ) and rigidity ( $\omega$ ) decrease with increasing density for steam and mesophase densities below PA; both increase with density for the liquid phase above a minimum near to  $\rho_{PA}(T_c)$ . The RS line,  $\omega = RT$  is more convenient reference point in describing equations-of-state and Gibbs energies for phase transitions. Its derivative,  $\sigma$ , Equation (8), is negative for a gas, zero in the mesophase, and positive for liquid-side states. Equations (6)-(8) show that there must exist a maximum coexisting gas-phase density along the percolation line PB, and minimum coexisting liquid density, respectively, since both  $w(T)$  and  $\sigma(T)$  go to zero at  $T_c$ .

For all terms  $n > 3$  negligible, all points on the gas-phase percolation line PB, including the maximum coexisting gas density at  $T_c$ , occur when  $\sigma$  is zero in Equation (8), and PA, including minimum coexisting liquid density, likewise, can be obtained from  $w$  is a minimum in Equation (6).

$$3\rho_{PB}(T) = 2\rho_{PA}(T) = -(b_2/b_3)_T \quad (9)$$

For the coexisting densities at  $T_c$ , Equation (9) can be shown to be very close to experimental reality. We can calculate the ratio  $-(b_2/3b_3)_T$  [19] over a range of  $T$  from  $T_c$  to  $T_b$ . Preliminary results are shown in **Figure 9**. Over this temperature range, the BW line can be represented by a single ground-state density constant that determines  $-(b_2/3b_3)_T$  more accurately by using the limiting region  $T \rightarrow T_b$ , a result first noted by Powles [12].

Thus, if the terms  $b_n > 3$  in Equations (9) and (10) are negligible for the gas phase below the PB line, the result can be used to confirm the experimental observation that the  $\omega$  goes to a constant and that the solidity ( $\sigma$ ) goes to zero at  $-(b_2/3b_3)_T$ . The virial ratio value at  $T_c$  is obtained from **Figure 8** at the zero-density intercept  $-(b_2/b_3)_0 = -0.1162T + 50$  mol/l. This is accurate to within the uncer-

tainty that we can extract the values in **Figure 8** from the NIST data [7], as 3-times the maximum reported experimental coexisting gas density (ca. 16 mol/l) and minimum coexisting liquid density (ca. 22 mol/l) as seen in **Figure 1**, **Figure 2**, **Figures 4-6**, from PB and PA at  $T_c$ .

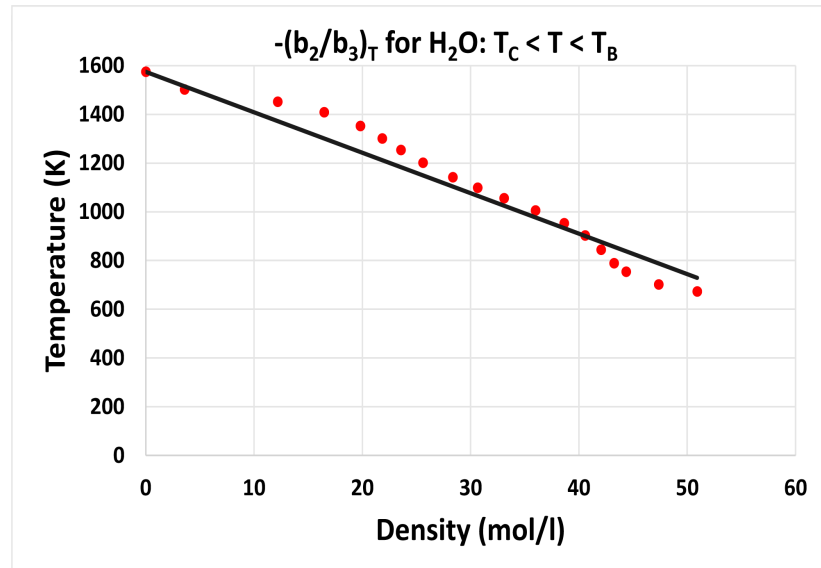


**Figure 9.** The ratio  $-(b_2/b_3)_T$  data points (red) from NIST H<sub>2</sub>O isotherms [7]: the value is zero at the Boyle temperature (1567 K) and, to within the present level of uncertainty, the data is consistent with an equivalence with the Boyle line  $\rho_{BW}(T)$  (black) for  $T > T_c$ .

Likewise, Equation (6) for the BW line can be used to obtain the minimum coexisting water density. From **Figure 5**, the Boyle-work  $w(\rho)_T$  goes to a minimum at the density  $\rho_{PA}(T_c)$ . Then,  $b_2 + b_3\rho_{PA} = 0$  at  $T_c$ , resulting in the simple equality again that the minimum coexisting liquid density at  $T_c$  is given by  $\rho_{PA}(T_c) = -1/2 (b_2/b_3)_{T_c}$ . Using the ground-state constant 82.8 mol/l to define the  $T_B$  asymptotic slope of  $-(b_2/b_3)_T$  data in **Figure 9**, we obtain a value  $\rho_{PA}(T_c) = 21.5$  mol/l. This result is also reassuringly close to the values we have obtained from NIST thermodynamic steam water coexistence data [7] in **Figure 1**, **Figure 2**, **Figures 4-6**.

## 4. Liquid State Virial Expansions

### 4.1. Relationship between BW and RS Lines

The condition  $(p/\rho_{BW})_T = RT$  defines the BW line that connects all these state points of both the super- and sub-critical liquid along any isotherm below  $T_B$ . The linearity can be explained by considering the form of a rigidity symmetry line. The RS line, defined by Equations (1) and (10)  $\omega(T) = RT$  has its origins in the symmetry of gas and liquid density fluctuations which are equivalent to ideal gas density variance along this line in accord with Equation (1). Again, from the rigidity virial expansion Equation (10) for H<sub>2</sub>O we see a simple prediction. If the isotherm were to be perfectly symmetric, then the virial expansion that defines the rigidity for the gas below PB-line can be applied for liquid-state densities between the PA-

percolation line and the rigidity symmetry line  $\rho_{RS}(T)$ . Then, the rigidity for  $\rho_{PA} < \rho < \rho_{RS}$

$$\omega = RT \left( 1 + 2b_2\Delta\rho + 3b_3\Delta\rho^2 + \dots + nb_n\Delta\rho^{n-1} \right) \quad (10)$$

where  $\Delta\rho = (\rho_{RS} - \rho)_T$ . The RS line  $\rho_{RS}(T)$ , when  $\Delta\rho = 0$ , decreases linearly with  $T$ . Along any isotherm the symmetry (**Figure 5**) extends to the BW line density  $\rho_{BW}(T)$ . Since, for all densities beyond  $\rho_{PA}(T)$ , there are no phase transitions of any order, both the Boyle-work ratio  $w(T)$  and rigidity  $\omega(T)$  are continuous in all their density derivatives along the respective lines to the first-order phase transitions on condensation. If all the higher terms  $n \geq 4$  in Equations (6)-(8) are negligible by cancellation for densities below  $\rho_{PB}$ , then, for the Boyle work ratio

$$w = RT \left( 1 + b_2\Delta\rho + b_3\Delta\rho^2 \right) \quad (11)$$

where  $\Delta\rho = (\rho_{BW} - \rho)_T$ . Then from (10) and (11), neglecting all  $b_n$  terms  $n > 3$ ,

$$\rho_{RS}(T) = 2\rho_{BW}(T)/3 \quad (12)$$

Equation (12) suggests that the BW line ( $p/\rho_B = RT$ ) will relate to the RS line for all supercritical liquid-side states. For  $H_2O$ , as with argon [15], this simple relationship between BW and RS lines is found to be in accord with the experimental  $p(\rho, T)$  data.

## 4.2. Fluid Phase Diagram

Using the experimental co-existence envelope data from NIST [9], for the present, we can construct an accurate phase diagram that enables the bounds of the  $p(\rho, T)$  equations-of-state to be quantified. There are no arbitrary parameters other than the virial coefficients  $b_2(T)$  and  $b_3(T)$  and the physical constants that they determine. The Boyle temperature  $T_B$  is determined by  $b_2(T)$ : when it changes sign from negative to positive. The BW line ground state density is then equivalent to the  $(-b_2/b_3)_T$  line.

This ground-state constant, determined also from the virial coefficients, can be used to sketch an accurate fluid-state diagram using the various simple equalities derived above. The ratio  $-(b_2/b_3)_T$ , below  $T_B$ , determines the BW line ground-state constant for water. Given the simple relationships between PA, PB, RS, and BW for all isotherms  $T < T_B$ , we can determine the critical temperature  $T_c$  (whence  $w(T) \rightarrow$  zero at  $\rho_{PA}(T)$  or  $\rho_{PB}(T)$ , and then fill in the isotherms of  $p(T)$ ,  $w(T)$ , or  $\omega(T)$  over the temperature range from the triple point to the BW line and beyond, to the state points above the BW line below  $T_B$  (**Figure 10**). At lower temperatures below  $T_c$ , water has a curved Boyle work line [20]. The Boyle line ( $T > T_c$ ) bifurcates below the linear  $-(b_2/b_3)_T$  value at a density around 55 mol/l at a temperature below  $T_c$  around 600 K.

The second observation from the water-steam delineated phase diagram is that the equilibrium regions of the BW and RS lines completely exist only within a single Gibbs supercritical “liquid” phase with  $P = 1$ . Whereas the percolation

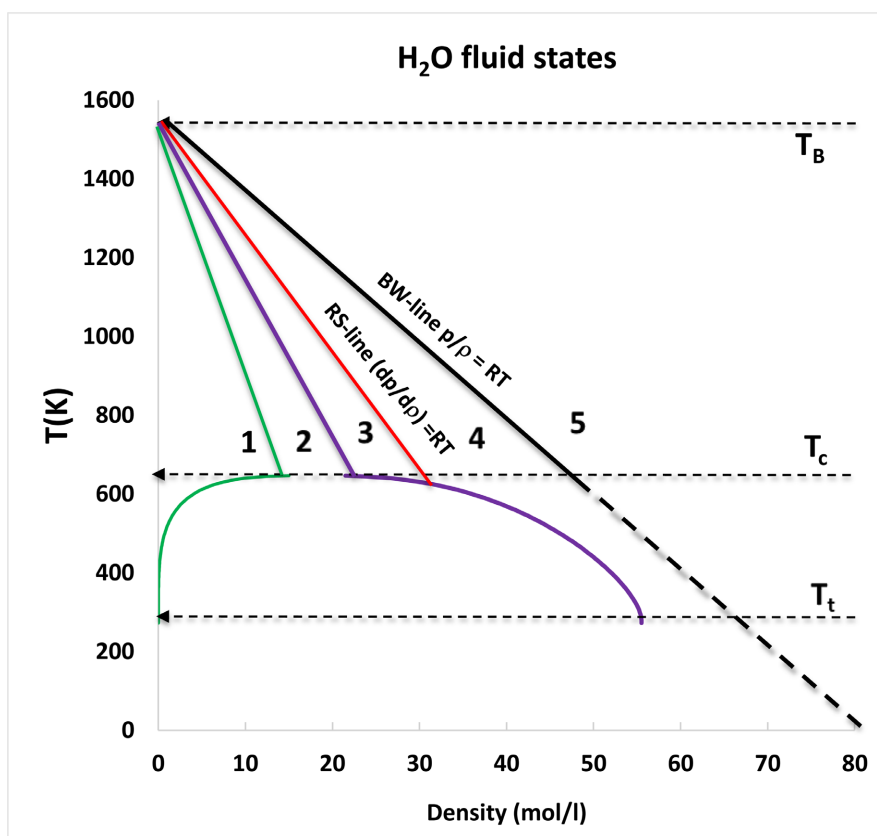


**Figure 10.** Temperature-density phase diagram of fluid states of steam and water: the equilibrium mesophase defined by the percolation loci PB and PA, shown as green and lilac lines respectively: both Boyle-work  $\rho_{BW}(T)$  and rigidity symmetry  $\rho_{PB}(T)$  and  $\rho_{PA}(T)$ , are  $\rho_{RS}(T)$  are linear in the equilibrium one-phase supercritical region and relate in accord with equation (12):  $T_B = 1567$  K (from **Figure 4**) and the dashed BW interpolation defines the H<sub>2</sub>O-BW ground-state constant  $\rho_{BW}(0) = 82.8$  mol/l (from **Figure 4**).

transitions delineate the supercritical gas and liquid regions by higher-order phase transitions, the BW and RS lines have no phase transitions and are therefore continuous in all their derivatives and the expansions of Equations (10)-(12) for the liquid-side of the mesophase are exact in the vicinity of BW and RS lines and accurate over the range of the respective regions in **Figure 9**. Since both lines are defined by their ground-state physical constant densities obtained in linear interpolation limit that  $T \rightarrow 0$ , but given  $T_B$  and  $T_c$ , only  $\rho_{BW}(0)$  is required to determine PB, PA, RS, BW(T) and given  $b_2(T)$  then  $\rho_{BW}(0)$  also determines  $b_3(T)$  for use in virial equations-of-state.

## 5. Conclusions

We conclude that in calculating the thermodynamic properties from an equation-of-state for water and steam the use of *ad hoc* delineation lines in the  $p$ - $T$  plane in the 5 regions in **Figure 3** requiring a numerical *tour de force* with 148 adjustable parameters may be unnecessary. By contrast, given the science of symmetry between gas and liquid states,  $p$  can be represented in the  $\rho$ - $T$  plane with zero *ad hoc*

adjustable parameters. An accurate knowledge of the three characteristic Boyle, critical and triple-point temperatures, and just 1 other physical constant, namely the ground state BW-line density  $\rho_{BW}(T \rightarrow 0)$  suffices. This remarkable simplification is a consequence of a fundamental symmetry between steam and water states on either side of a critical divide, supercritical mesophase, and subcritical 2-phase fluid coexistence regions.

The Boyle-line ground-state constant  $\rho_{BW}(0)$  ( $\approx 82.5$  mol/l) is found to play a pivotal role in formulating an equation-of-state, from a general statistical theory, that gives rise to the phenomenological symmetry we have reported. It is in the range of the most stable crystal structures as  $T \rightarrow 0$ . The Boyle density constant we obtain for steam-water, would, at first sight, appear to have no thermodynamic status. The maximum density of Ice1 (c or h) is around 55 - 60 mol/l. Water, however, albeit ubiquitous, is the most complex of molecular fluids. Its ice solid states can have up to 16 or more different stable structures in the equilibrium phase diagrams. The highest known crystalline ice density was discovered 60 years ago [21] as ice VII, around 94 mol/l. Alongside the argon FCC maximum packing result [15], this is a curious conundrum. These results suggest a thermodynamic relationship, presently inexplicable, between the limiting “zero density expansion” Mayer virial coefficients for steam, and an ice minimum energy ground state  $T \rightarrow 0$ .

Finally, it needs to be emphasized that this is a preliminary conference presentation summary of results to date for H<sub>2</sub>O. Our research is on-going; the next stage for an *ad hoc* parameter-free model for water is to verify the accuracy by comparison with the experimental data. We are also developing a parameter free gas-liquid science-based coexistence line, and more accurate representations of the virial coefficients  $b_3(T)$  and  $b_4(T)$  for water, from the experimental  $p(\rho, T)$  literature that have hitherto been unavailable at the required accuracy.

## Acknowledgements

This research has been conducted under the auspices of an EU-ERASMUS MSc. by Dissertation Research Studentship Award 2023-24 to Ahmad Eltahlawi to be submitted at the University of Algarve 2025.

## Conflicts of Interest

The authors declare no conflicts of interest regarding the publication of this paper.

## References

- [1] Gibbs, J.W. (1928) Chapter II: Equilibrium of Heterogeneous Phases. *Transactions of the Connecticut Academy of Arts and Sciences*, **2**, 309-342.
- [2] van der Waals, J.D. (1873) On the Continuity of the Gaseous and Liquid States (in Dutch). Ph.D. Thesis, University of Leiden.
- [3] Sandler, S.I. and Woodcock, L.V. (2010) Historical Observations on Laws of Thermodynamics. *Journal of Chemical & Engineering Data*, **55**, 4485-4490.

- <https://doi.org/10.1021/je1006828>
- [4] Gibbs, J.W. (1928) Chapter III: Critical Phases. *Transactions of the Connecticut Academy of Arts and Sciences*, **3**, 343-524.
- [5] Maguire, J.F. and Woodcock, L.V. (2023) Hypotheses in Phase Transition Theories: What Is 'liquid'? *Journal of Molecular Liquids*, **373**, Article 121199. <https://doi.org/10.1016/j.molliq.2023.121199>
- [6] Wilson, K.G. (1993) The Renormalization Group and Critical Phenomena. December 8, 1982, Nobel Lectures, Physics 1981-1990. World Scientific Publishing.
- [7] NIST (2024) Thermophysical Properties of Fluid Systems in Chemistry Webbook. <https://webbook.nist.gov/chemistry/fluid/>
- [8] Wagner, W. and Pruß, A. (2002) The IAPWS Formulation 1995 for the Thermodynamic Properties of Ordinary Water Substance for General and Scientific Use. *Journal of Physical and Chemical Reference Data*, **31**, 387-535. <https://doi.org/10.1063/1.1461829>
- [9] Wagner, W. and Kretzschmar, H.-J. (2019) International Steam Tables: Properties of Water and Steam Based on the Industrial Formulation IAPWS-IF97. 3rd Edition, Springer.
- [10] Woodcock, L.V. (2013) Observations of a Thermodynamic Liquid-Gas Critical Coexistence Line and Supercritical Fluid Phase Bounds from Percolation Transition Loci. *Fluid Phase Equilibria*, **351**, 25-33. <https://doi.org/10.1016/j.fluid.2012.08.029>
- [11] Khmelinskii, I. and Woodcock, L. (2020) Supercritical Fluid Gaseous and Liquid States: A Review of Experimental Results. *Entropy*, **22**, 437-463. <https://doi.org/10.3390/e22040437>
- [12] Powles, J.G. (1983) The Boyle Line. *Journal of Physics C: Solid State Physics*, **16**, 503-514. <https://doi.org/10.1088/0022-3719/16/3/012>
- [13] Apfelbaum, E.M. and Vorob'ev, V.S. (2020) The Line of the Unit Compressibility Factor (Zeno-Line) for Crystal States. *The Journal of Physical Chemistry B*, **124**, 5021-5027. <https://doi.org/10.1021/acs.jpcc.0c02749>
- [14] Woodcock, L.V. (2016) Thermodynamics of Gas-liquid Criticality: Rigidity Symmetry on Gibbs Density Surface. *International Journal of Thermophysics*, **37**, 24-40. <https://doi.org/10.1007/s10765-015-2031-z>
- [15] Woodcock, L.V. (2024) Rigidity Symmetry Line for Thermodynamic Fluid Equations-of-State. *Journal of Modern Physics*, **15**, 613-633. <https://doi.org/10.4236/jmp.2024.155029>
- [16] Hansen, J.-P. and Macdonald, I.R. (2013) Theory of Simple Liquids. 4th Edition, Elsevier.
- [17] Sedunov, B. (2008) Monomer Fractions in Real Gases. *International Journal of Thermophysics*, **11**, 1-9. <https://doi.org/10.1155/2012/859047>
- [18] Harvey, A.H. and Lemmon, E.W. (2004) Correlation for the Second Virial Coefficient of Water. *Journal of Physical and Chemical Reference Data*, **33**, 369-376. <https://doi.org/10.1063/1.1587731>
- [19] Eltahlawy, A. (2025) Equation-of-State for Water. Masters' Dissertation, University of Algarve.
- [20] Mayrhuber, F. (2021) Analysis of P, T, P-Data for All Fluid States via Comparison with a Transcribed Van Der Waals Equation. *Chemical Thermodynamics and Thermal Analysis*, **1**, Article 100003. <https://doi.org/10.1016/j.ctta.2021.100003>
- [21] Kamb, B. and Davis, B.L. (1964) ICE VII, the Densest Form of Ice. *Proceedings of the National Academy of Sciences*, **52**, 1433-1439. <https://doi.org/10.1073/pnas.52.6.1433>